

Adaptive speed control for drives with variable moments of inertia and natural frequencies

Dipl.-Ing. Fabian Mink, LTi DRIVES GmbH Lahnau, Entwicklung Software Dr.-Ing.
Alexander Bähr, LTi DRIVES GmbH Lahnau, Entwicklung Software

Adaptive speed control for drives with variable inertia and resonance frequency

In order to obtain high performance control of an industrial servo drive, speed control parameters need to be matched exactly to the mechanical properties of the drive. Basically, the drive's mechanical system can be time-variant. Online adaption is necessary to keep dynamics of the controlled system constant. For the determination of PI speed control gain the drive's inertia has to be taken into account. To avoid excitation of mechanical resonances by the speed controller, a notch filter may be inserted in the speed control loop which can help to suppress oscillation.

In this paper, auto-tuning methods for speed control gain and notch filter are presented.

Speed control, adaptive, auto-tuning, inertia, resonance frequency

1. Introduction

In order to meet demands for fast cycle times and improved precision of production machinery, drive controllers need to be adapted exactly to the machine mechanics. Since the behaviour of the mechanics may be time-variant, online adaption is necessary.

In doing so, the speed controller must adjust to a variable moment of inertia in order to attain a constant dynamics. The difficulty lies in precise determination of the moment of inertia, in particular under the influence of friction, load and other non-modellable disturbances. To resolve this, a method based on a state observer is presented. If a moment of inertia is incorrectly parameterised, the observer exhibits characteristic observer (position) errors which are correlated with the jerk of the axle.

In order to prevent amplification of mechanical oscillations by the speed control loop, an adaptive notch filter can be installed in the speed controller. The middle frequency of the filter must be optimised depending on the mechanical resonance. To do so, a method is presented which tunes the center frequency adaptively to the oscillation frequency in the control loop.

The methods presented have been implemented in the software of the LTi DRIVES ServoOne servocontroller.

2. Model of the mechanism

2.1 One-mass system (OMS), rigid mechanics

The model described in the following is used to adapt to a variable inertia. The starting point is a rigid, mechanically non-oscillating mechanics. The torque M_{Mot} generated by the motor is counteracted by friction M_{Fric} and an external load torque M_{Load} . The friction is modelled by a direction-dependent (dry friction) component and a speed-dependent (viscose friction) component:

$$M_{Fric} = \mu \cdot \text{sign}(\omega) + \eta \cdot \omega \quad (1)$$

In this, μ and η are the corresponding friction coefficients. The model of the mechanism is shown in figures 1a/b.

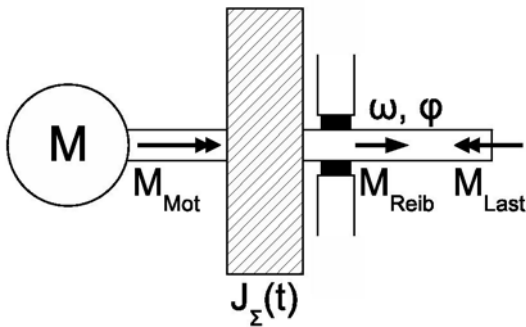


Figure 1a: One-mass model of the mechanics

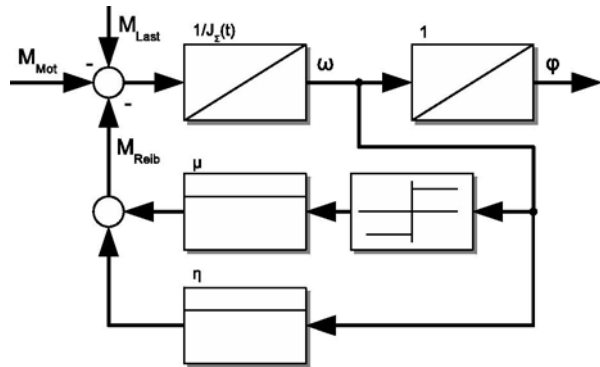


Figure 1b: Equivalent circuit diagram of the control system

Legende:

Last = Load

Reib = Fric

Applying the principle of angular momentum, with the total inertia $J_{\Sigma}(t)$ of the drive the following differential equations result (ω is the mechanical angular velocity, ϕ the mechanical angle of rotation, assuming $j_{\Sigma}(t) \cdot \omega$ low):

$$\phi = \omega \quad (2a)$$

$$J_{\Sigma}(t)\omega + \mu \cdot \text{sign}(\omega) + \eta \cdot \omega + M_{Load} = M_{Mot} \quad (2b)$$

2.2 Two-mass system (TMS), mechanism with one resonance frequency

If the drive is operated with high dynamics, it is no longer permissible to view it as a rigid system. In a first approximation, the mechanics can then be viewed as a dual-mass system. Consequently, precisely one resonance frequency is modelled. Additional resonances may also occur in the drive (higher-order multi-mass system). The elasticity is modelled by a linear torsion spring:

$$M_{12} = c_f \cdot (\phi_{Mot} - \phi_{Load}) + d_f \cdot (\omega_{Mot} - \omega_{Load}) \quad (3)$$

The model of the mechanics is shown in figure 2.

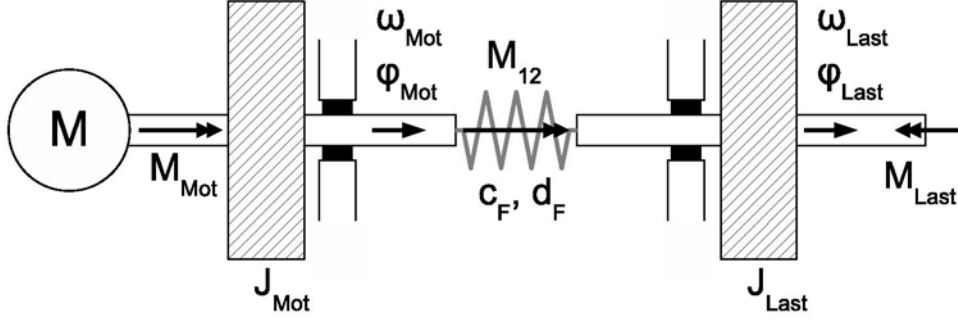


Figure 2: Two-mass model of the mechanics

Thus for the system of differential motion equations the results are the following state space matrices (state vector $\underline{x} = (\varphi_{Mot}, \omega_{Mot}, \varphi_{Load}, \omega_{Load})^T$, input vector $\underline{u} = (M_{Mot}, M_{Load})^T$, $\dot{\underline{x}} = \underline{A} \cdot \underline{x} + \underline{B} \cdot \underline{u}$):

$$\underline{A} = \begin{pmatrix} 0 & 1 & 0 & 0 \\ -\frac{c_f}{J_{Mot}} & -\frac{d_f}{J_{Mot}} & \frac{c_f}{J_{Mot}} & \frac{d_f}{J_{Mot}} \\ 0 & 0 & 0 & 1 \\ \frac{c_f}{J_{Load}} & \frac{d_f}{J_{Load}} & -\frac{c_f}{J_{Load}} & -\frac{d_f}{J_{Load}} \end{pmatrix} \quad \underline{B} = \begin{pmatrix} 0 & 0 \\ \frac{1}{J_{Mot}} & 0 \\ 0 & 0 \\ 0 & -\frac{1}{J_{Load}} \end{pmatrix} \quad (4)$$

Definitions are given for the variables total inertia J_Σ , mass ratio V_J , characteristic radian frequency ω_0 , relative damping d , natural frequency ω_e , and resonance frequency ω_{res} :

$$J_\Sigma = J_{Mot} + J_{Load} \quad (5a) \quad \omega_0 = \sqrt{c_f} \cdot \frac{J_\Sigma}{J_{Mot} \cdot J_{Load}} \quad (5c) \quad \omega_e = \omega_0 \cdot \sqrt{1-d^2} \quad (5e)$$

$$V_J = \frac{J_{Load}}{J_{Mot}} \quad (5b) \quad d = \omega_0 \cdot \frac{d_f}{2c_f} \quad (5d) \quad \omega_{res} = \omega_0 \cdot \sqrt{1-2d^2} \quad (5f)$$

It is assumed that d is low, resulting in a response capable of oscillation. The transfer function in the Laplace domain can be derived thus:

$$G_{DMS}(s) = \frac{\omega_{Mot}(s)}{M_{Mot}(s)} = \frac{1}{sJ_\Sigma} \cdot \frac{1 + 2\frac{d}{\omega_0}s + \frac{V_J+1}{\omega_0^2}s^2}{1 + 2\frac{d}{\omega_0}s + \frac{1}{\omega_0^2}s^2} \quad (6)$$

The magnitude of the frequency response has a characteristic maximum (resonance) and a minimum (anti-resonance).

A dual-mass system is likewise created when the position or speed encoder is not coupled ideally rigidly to the drive mechanics. The encoder inertia can be assumed to be very low relative to the drive's moment of inertia. The speed is then measured on the load side. The result is a purely PT₂ response:

$$G_{Encoder}(s) = \frac{\omega_{Meas}(s)}{\omega_{Mot}(s)} = \frac{1}{1 + 2\frac{d_G}{\omega_G}s + \frac{1}{\omega_G^2}s^2} \quad (7)$$

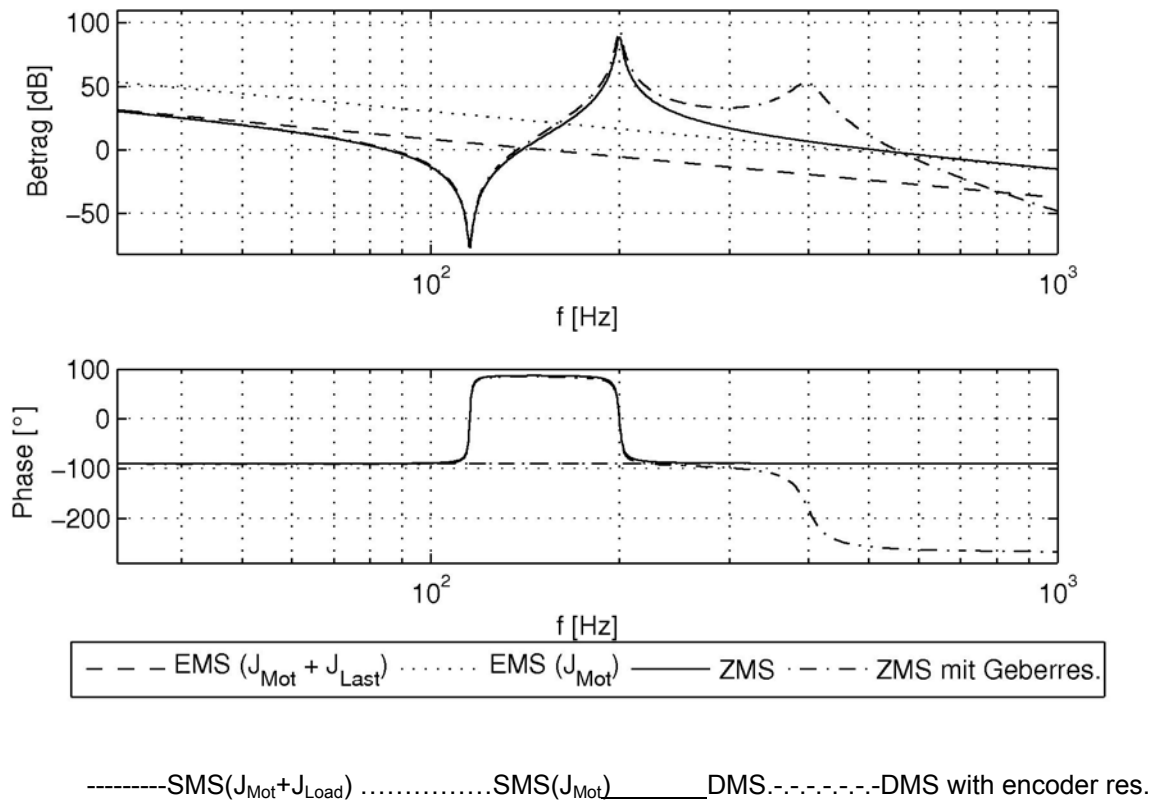


Figure 3: Frequency responses of different mechanical structures

Legende:

Betrag = Amount

Phase = Phase

Figure 3 shows frequency responses of various systems. At low frequencies well below anti-resonance, the DMS behaves like a SMS of the same overall inertia. Above the resonance the load mass is "decoupled". The controller only "sees" the motor-side mass.

3. Speed control loop

The speed control loop of an industrial servocontroller is shown in figure 4. For the sake of simplicity, PT_1 behaviour is assumed for the underlying current control loop.

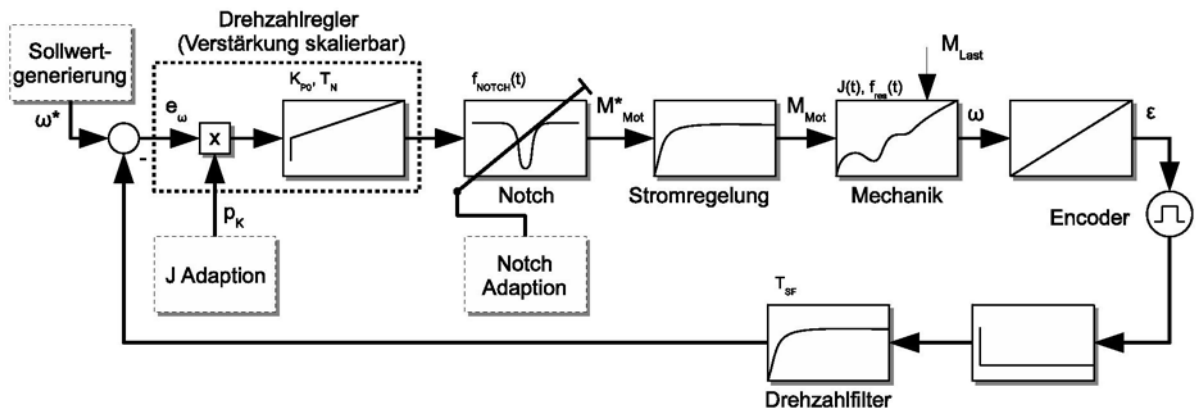


Figure 4: Speed control loop of an industrial servocontroller

Legende:

- Drehzahlregler = Speed controller
- Drehzahlfilter = Speed filter
- Last = Load
- Mechanik = Mechanism
- Sollwertgenerierung = Setpoint generation
- Stromregelung = Current control
- Verstaerkung skalierbar = Gain scaleable

The gain K_P of the speed controller is scaleable. A notch filter is provided in the control loop; the filter frequency can be changed online.

4. Adaption to variable mass moment of inertia

If the moment of inertia of the drive changes during operation while the controller gain remains constant, a change occurs in the dynamics of the closed control loop.

If the inertia decreases, the magnitude of the transfer function of the open control loop is increased - the closed control loop is increasingly taken to its stability limit. In extreme cases the control system may become unstable. If the inertia increases, this results in a larger control deviation (speed lag error) at constant acceleration, as now a larger control variable (torque) is required. The dynamism decreases. Ideally therefore, the controller gain is adapted to a change in the inertia with the same scaling. The change in J is then shortened against the change in K_P in the transfer function of the control loop. The most precise possible knowledge of the moment of inertia is also advantageous for balancing of any torque pre-control, or to adapt the positioning profiles (acceleration).

In [6] a method is presented based on a state observer for a single-mass model of the controlled system. The inertia is adapted by evaluating an observed disturbance torque. If the inertia in the system model of the observer deviates from the actual inertia, this correlates to the acceleration of the axle. In the method presented here, the estimated position error of the observer is used for adaption purposes. If the inertia in the system model of the observer deviates, this correlates to the jerk of the axle.

4.1. State observer

The state observer used comprises a single-mass model of the mechanics and a feedback loop of the observer error. The friction is not modelled. This results in a very simple observer structure, which is shown in figure 5.

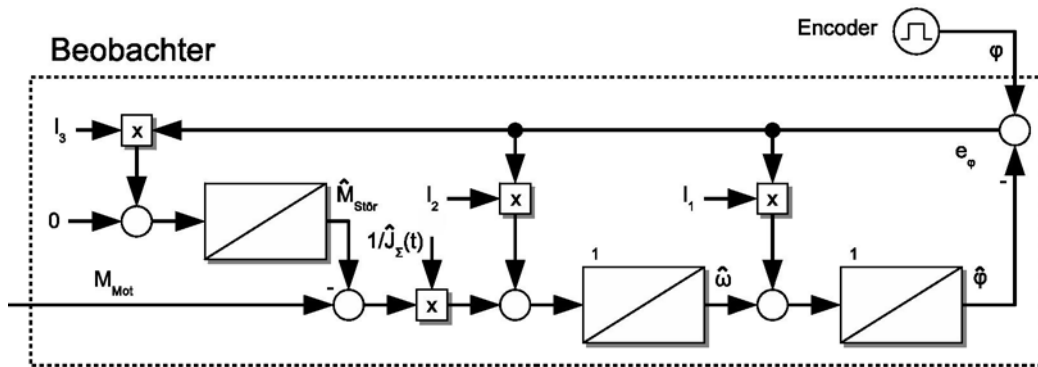


Figure 5: State observer with disturbance observation for an OMS

Beobachter = Observer

The observer can be described as follows in the state space (state vector: $\underline{x}_B = (\overline{\varphi}, \overline{\omega}, \overline{M}_{Dist})^T$):

$$\dot{\underline{x}}_B = \underline{A}_B \cdot \underline{x}_B + \underline{B}_B \cdot u + \underline{l} \cdot e_\varphi \quad \underline{A}_B = \begin{pmatrix} 0 & 1 & 0 \\ 0 & 0 & -\frac{1}{\hat{J}_\Sigma} \\ 0 & 0 & 0 \end{pmatrix} \quad \underline{B}_B = \begin{pmatrix} 0 \\ 1 \\ \hat{J}_\Sigma \\ 0 \end{pmatrix} \quad \underline{l} = \begin{bmatrix} l_1 \\ l_2 \\ l_3 \end{bmatrix} \quad u = M_{Mot} \quad (8)$$

The configuration of the observer - i.e. the determination of \hat{I} - is effected by means of cross ratios [1]. To do this an equivalent time constant T_B must be specified, for which around $T_B = 10\text{ms}$ has proved effective. The observer thus settles in about 30-50ms.

The response of the observer to disturbing influences is shown in figures 6a/b (simulation). While the estimated disturbance torque in motion also reacts to viscose and dry friction torques, a marked observer error is shown primarily where the assumed inertia is incorrect. A robustness to friction and load torques is produced. In this case the observer error correlates to the jerk of the axle (change in acceleration).

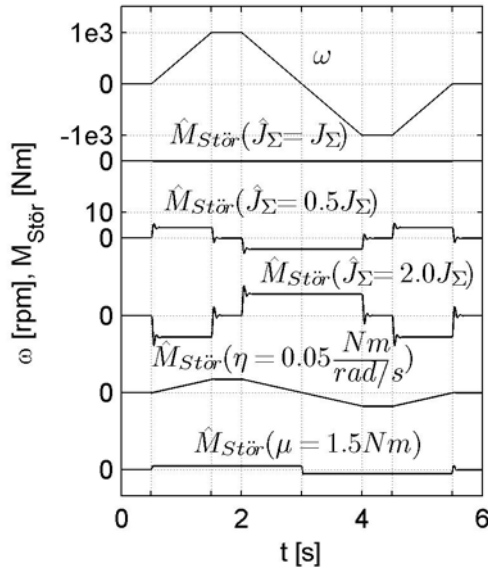


Figure 6a: Disturbance torque estimation

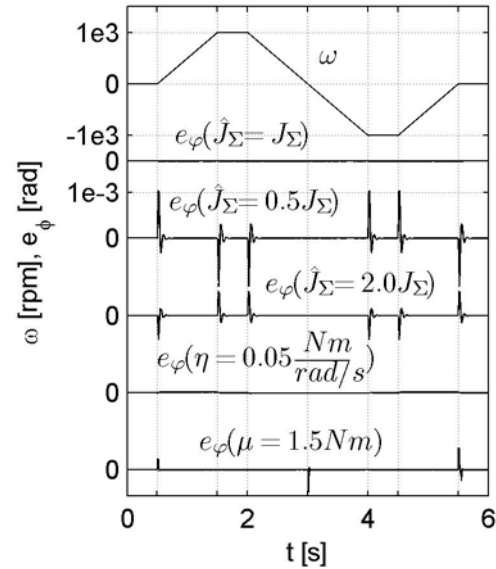


Figure 6b: Observer error

Legende:

Stör = Dist

4.2. Adaption method

The correlation between observer error e_ϕ and jerk j is utilised for an adaption of the estimated inertia. For this, the jerk is generated from the speed setpoint and then with a mean value filter (length T_j) "stretched" to the settling time of the observer.

After multiplication (correlation) by the observer error, the adaption signal is fed in. Scaling of the moment of inertia to the originally assumed value has proved effective (scaled inertia p_J):

$$\hat{J}_\Sigma(t) = p_J(t) \cdot \hat{J}_{\Sigma 0}, \hat{J}_{\Sigma 0} \text{ is the originally assumed inertia} \quad (9)$$

The adaption rate can be adjusted by way of the adaption constant λ_J and is also adapted to the current estimate: If p_J is high, larger step widths are applied in the adaption process than if it is low. The following adaption equation ($p_J(k) = p_J(k \cdot T_s)$) results:

$$p_J(k+1) = p_J(k) + p_J(k) \cdot \lambda_J \cdot (j_{\text{fit}} \cdot e_\phi) \quad (10)$$

The scaling offers the additional advantage that the gain K_P can be adjusted with the same scale to attain the desired constant dynamism of the speed control loop - an additional upstream PT_1 element ($TK \approx 1\text{s}$) prevents step changes in the speed controller gain (scaled gain p_K):

$$K_p(t) = p_K(t) \cdot K_{p0} \text{ where } p_K(s) = p_J(s) \cdot \frac{1}{1 + sT_K} \quad (11)$$

The adaption is presented in the block diagram in figure 7.

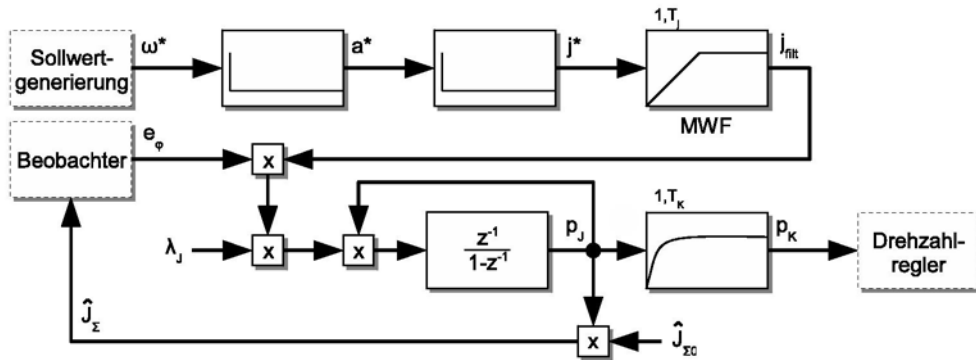


Figure 7: Block diagram: Adaption to variable mass inertia.

Legende

Sollwertgenerierung = Setpoint generation

Beobachter = Observer

Drehzahlregler = Speed controller

MWF = MVF

5. Adaptive notch filter

A variety of methods are conceivable to reduce unwanted oscillations caused by mechanical resonances. The use of an adaptive notch filter in the speed control loop is a very simple method requiring minimal knowledge of the controlled system. [4]

The notch filter must be tuned to an occurring oscillation in the control loop. To determine the oscillation frequency, FFT-based methods have been extensively propagated to date in the literature. [4], [5]

An alternative possibility for detecting resonances in read head drives of hard disks is presented in [3]. To do this, the control signal is routed through two band-pass filters - one of which has a center frequency below the currently assumed resonance and one above it. By comparing the signal energy at the outputs of the two filters, an indication can be obtained as to whether the resonance needs to be assumed higher or lower. This makes it possible to adapt the frequency. No memory-intensive signal buffers are required; the necessary computing power is much less than for a FFT.

5.1. Notch and band-pass filters

The filters used are specified as time-continuous, and are translated into time-discrete representation by means of bilinear transformation (IIR implementation).

With regard to the transfer function of the notch filter (middle frequency ω_N , quality Q):

$$G_N(s) = \frac{1 + \frac{1}{\omega_N^2} s^2}{1 + \frac{1}{Q_N \omega_N} s + \frac{1}{\omega_N^2} s^2} \quad (12)$$

The band-pass filters are of the 4th order, in order to attain adequate edge steepness (Butterworth filters, middle frequency ω_c , bandwidth ω_Δ):

$$G_{BP}(s) = \frac{s^2}{\frac{\omega_c^4}{\omega_\Delta^2} + \sqrt{2} \frac{\omega_c^2}{\omega_\Delta} s + \left(1 + 2 \frac{\omega_c^2}{\omega_\Delta^2}\right) s^2 + \sqrt{2} \frac{1}{\omega_\Delta} s^3 + \frac{1}{\omega_\Delta^2} s^4}$$

5.2. Adaption method

The measurement signal used is the control difference from the speed control loop. It is routed through the two band-pass filters BP_L and BP_H , at the outputs of which energy quantities are respectively calculated by squaring and subsequent integration. At fixed time intervals the output energies are sampled, the difference between them formed and the integrators reset. The filter frequency is adapted up or down according to the preceding sign. The two band-pass filters are likewise adapted. The rate of frequency change is dictated by an adaption constant λ_{Notch} . By means of a parameterisable limitation Δf_{max} a maximum change per step can also be preset. The adaption method is presented in the block diagram in figure 8.

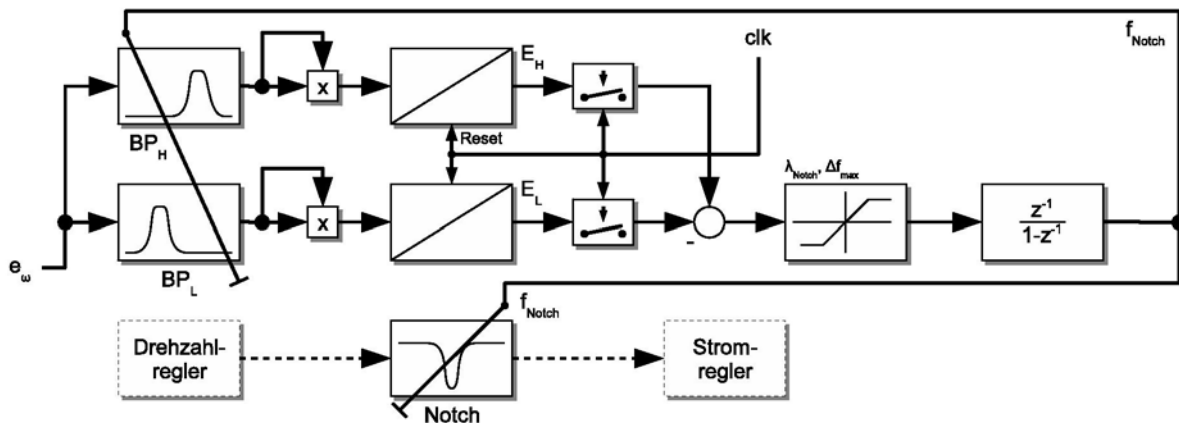


Figure 8: Block diagram of adaptive notch filter

Legende

Drehzahlregler = Speed controller

Stromregler = Current controller

Notch = Notch

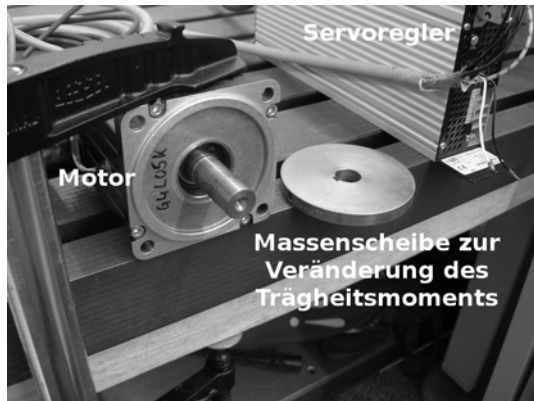
6. Measurement results

The measurements presented were performed on two different test set-ups. They are shown in figures 9a/b. For adaption to a variable inertia, a single motor is used and mass disks are bolted onto its shaft to provide a simple means of altering the inertia.

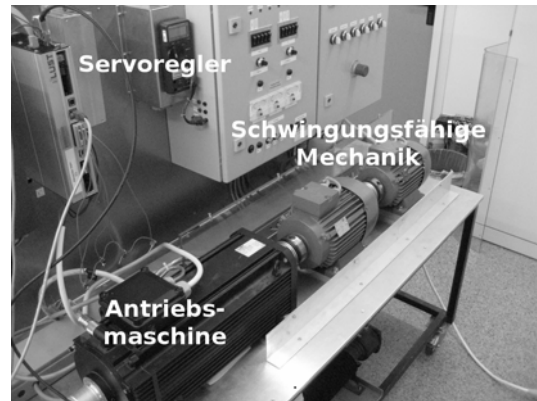
With the mass disk removed, the speed controller is rated with a bandwidth of around 40Hz^1 . After mounting the mass disk shown, the dynamism decreases and overshoot occurs (see figure 10). By activating the adaption, the estimated inertia adapts to roughly 7 times (p_J) the original value. The controller gain is also increased correspondingly (p_K), as a result of which the original dynamics is again attained.

¹ Was selected so that the overshoot is visible. Higher bandwidths up to around 200Hz are possible.

F



Trägheit Motor: $J_{Mot} = 1.0 \text{ kgcm}^2 = J_{\Sigma 0}$
 Trägheit Scheibe: $J_{Scheibe} = 6.7 \text{ kgcm}^2$
 Nennmoment: $M_N = 1.1 \text{ Nm}$
 Gebersystem: Resolver
 Drehzahlfilter: $T_{SF} = 1 \text{ ms}$



Trägheit Gesamt: $J_{\Sigma} = 370 \text{ kgcm}^2$
 Resonanzfrequenzen ca. $f_{res1} = 260 \text{ Hz}$,
 $f_{res2} = 550 \text{ Hz}$
 Nennmoment Antrieb: $M_N = 35 \text{ Nm}$
 Gebersystem: sinus/cosinus 512 Striche

Figure 9a: Test set-up for adaption to a variable inertia

Figure 9b: Test set-up for adaptive notch filter

Legende (Bild 9a & 9b):

- Antriebsmaschine = Drive machine
- Drehzahlfilter = Speed filter
- Gebersystem = Encoder system
- JScheibe = JDisk
- Massenscheibe zur ... = Mass disk to vary inertia
- Nennmoment = Rated torque
- Nennmoment Antrieb = Drive rated torque
- Resonanzfrequenzen ca. = Resonance frequencies approx.
- Schwingungsfähige Mechanik = Oscillating mechanism
- Servoregler = Servocontroller
- sinus/cosinus = sine/cosine
- Striche = lines
- Traagheit Gesamt = Total inertia
- Traagheit Motor = Motor inertia
- Traagheit Scheibe = Disk inertia

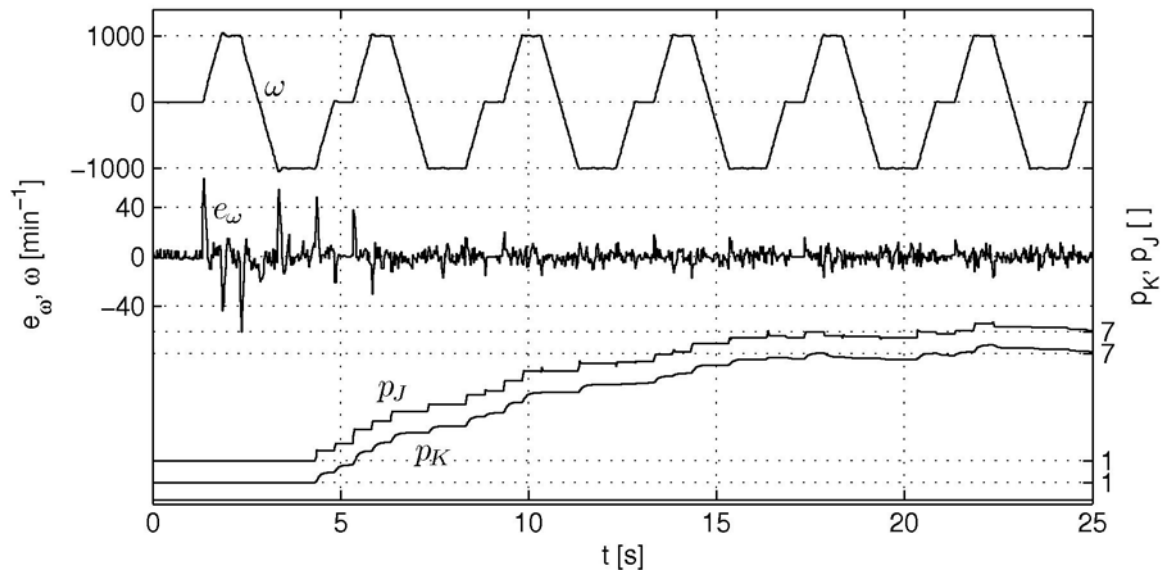


Figure 10: Adaption to a changed moment of inertia

The behaviour of the adaptive notch filter is demonstrated on a test rig with an oscillating mechanics (drive and load machines linked by bellows couplings). The controller configuration is oriented to the optimum damping (rated for the overall moment of inertia J_Σ). A mechanical resonance is strongly excited, the speed control loop is close to the stability limit (figure 11). By activating the algorithm, the filter frequency is adapted to the excited resonance. When this is reached, the oscillation is markedly damped.

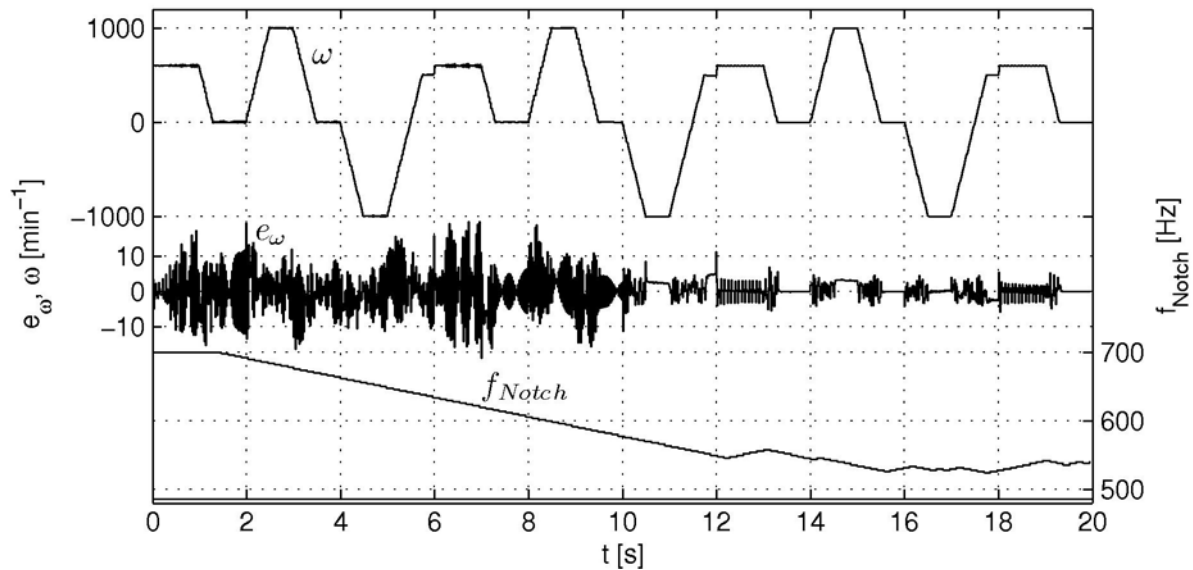


Figure 11: Adaption of the notch filter with mechanical resonance

7. Summary

With the adaption to a variable inertia and the adaptive notch filter, two methods were presented which enable the drive to be adapted to variable mechanical system parameters. In doing so, attention was paid to ease of implementation in an industrial servocontroller (including low computing power requirement). Both methods have been implemented in the LTi DRIVES ServoOne servocontroller. Adaption to a variable inertia proves particularly robust against friction and load torques, though rapid changes in acceleration are required in order to obtain good results. With the adaptive notch filter algorithm presented, the oscillation frequency of a resonance in the control loop can be determined without employing high-intensity computing methods (FFT). The notch filter is able to damp this oscillation to a large extent.

8. Literature

- [1] Beineke, Stephan; Bähr, Alexander: Observer-based Speed Estimation for Linear Motor Control. PCIM Europe 2006. [2] Beineke, Stephan: Online-Schätzung von mechanischen Parametern, Kennlinien und Zustandsgrößen geregelter elektrischer Antriebe [Online estimation of mechanical parameters, characteristics and state variables of loop-controlled electric drives]. Dissertation, Paderborn, 2000.
- [3] Ohno, Keitaro; Hara, Takeyori: Adaptive resonant mode compensation for hard disk drives. Transactions on Industrial Electronics Vol. 5, No. 2. IEEE, 2006.
- [4] Schmidt, Peter; Rehm, Thomas: Notch filter tuning for resonant frequency reduction in dual inertia systems. Industry Applications Conference, IEEE, 1999
- [5] Wang, Huijun; Lee, Dong-Hee; Lee, Zhen-Guo; Ahn, Jin-Woo: Vibration Rejection Scheme of Servo Drive System with Adaptive Notch Filter. PESC, IEEE 2006.
- [6] Yang Sheng-Ming; Deng, Yu-Jye: Observer-based Inertial Identification for AutoTuning Servo Drives. IAS. IEEE 2005.